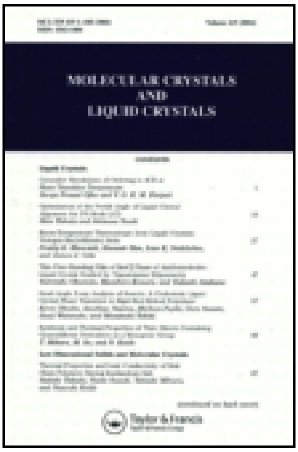

Molecular Crystals and Liquid Crystals

Publication details, including instructions for authors and subscription information:
http://www.tandfonline.com/loi/gmcl20

Theory-Inspired Nano-Engineering of Structure, Lattice Dimensionality, and Viscoelasticity of New Polymer and Dendrimer Materials

Larry R. Dalton [a] & Stephanie J. Benight [a]

[a] Department of Chemistry, University of Washington, Seattle, WA, 98195, USA

To cite this article: Larry R. Dalton & Stephanie J. Benight (2012): Theory-Inspired Nano-Engineering of Structure, Lattice Dimensionality, and Viscoelasticity of New Polymer and Dendrimer Materials, Molecular Crystals and Liquid Crystals, 554:1, 4-11

To link to this article: http://dx.doi.org/10.1080/15421406.2012.632733

Mol. Cryst. Liq. Cryst., Vol. 554: pp. 4–11, 2012
Copyright © Taylor & Francis Group, LLC
ISSN: 1542-1406 print/1563-5287 online
DOI: 10.1080/15421406.2012.632733

Theory-Inspired Nano-Engineering of Structure, Lattice Dimensionality, and Viscoelasticity of New Polymer and Dendrimer Materials

LARRY R. DALTON* AND STEPHANIE J. BENIGHT

Department of Chemistry, University of Washington, Seattle, WA 98195, USA

Moieties that promote intermolecular cooperativity are attached as pendants to organic electro-optic chromophores effecting a reduction in lattice dimensionality and influencing the poling-induced order of chromophores. Theory relates centric and acentric order parameters to lattice dimensionality. Experimentally, centric order parameters are defined by VAPRAS and VASE, while the acentric order parameters are extracted from ATR. Molecular cooperativity also influences viscoelastic properties. SM-FM demonstrates the existence of a distinct phase of matter of reduced dimensionality. IFA permits definition of the entropy change associated with the reduced dimensionality. The correlation of IFA and DRS data permits definition of the cooperativity length scale.

Keywords Lattice dimensionality ; nanoviscoelasticity; order parameters; organic electro-optic materials

Introduction

Organic electro-optic materials have the potential to dramatically improve device performances in telecommunication, sensing, and information technologies. However, in order to achieve this improved performance and eventually replace traditionally utilized inorganic materials, acentric order and electro-optic activity must be improved. The combination of time-dependent density functional theory (TD-DFT) and coarse-grained Monte Carlo/molecular dynamics (referred to as pseudo-atomistic Monte Carlo/molecular dynamics, PAMC/MD) has permitted quantitative analysis of the electric field poling-induced electro-optic activity for the following classes of organic electro-optic materials [1]: (1) chromophore-polymer composite materials [1–7], (2) chromophores covalently-incorporated into polymers and dendrimers [1,7–9], (3) binary chromophore materials [1,7,10], and (4) optically-poled binary chromophore materials [1,7,11]. For chromophore-polymer composite materials, poling-induced acentric order is defined by the competition of chromophore-chromophore dipolar interactions and chromophore-chromophore nuclear repulsive (steric) interactions. Adjustment of chromophore shape permits improvement of realizable electro-optic activity [12]. Such materials are essentially 3-D lattices. For chromophores covalently incorporated into polymers and dendrimers, it is important to take into account restrictions on chromophore reorientation under the influence of the poling field

---

*Address correspondence to Larry R. Dalton, Department of Chemistry, University of Washington, Seattle, WA 98195, USA. Tel.: (360) 981-4575; Fax: (206) 616-8602; E-mail: dalton@chem.washington.edu

that are associated with covalent bond potentials [1,8,9]. Such materials are also essentially 3-D lattice materials. The poling-induced order of binary chromophore materials, including those influenced by optical poling, is influenced by the interaction between guest and host chromophores [1,7,10,11,13]. This guest-host interaction leads to a reduction in lattice dimensionality since the poling-field reduces the lattice dimensionality of both guest and host chromophores and they influence each other through their intermolecular electrostatic interactions. A fifth class of materials, which has recently garnered significant interest, is matrix assisted poling (MAP) materials in which chromophores are covalently linked to pendant groups capable of strong intermolecular interactions. In this class of materials, the pendant groups restrict the possible orientations of the chromophore about its internal axis, therefore imposing a dimensional restriction. While the aforementioned theoretical methods have correlated this experimentally observed reduced dimensionality [14], these methods have yet to be utilized to study full molecular constructs of this class of materials.

The principal element of the electro-optic tensor for an electrically-poled organic electro-optic (OEO) material is given to good approximation by $r_{33} = N{<}\cos^3\theta{>}\beta_{zzz}f(\omega,\varepsilon)$ where N is the chromophore number density, $<\cos^3\theta>$ is the acentric order parameter, β_{zzz} is the principal element of the molecular first hyperpolarizability tensor, and $f(\omega,\varepsilon)$ is a local field factor depending on frequency (ω), dielectric permittivity (ε), and index of refraction (n). As shown in Fig. 1, a reduction in lattice dimensionality in the vicinity of electro-optic chromophores results in a significant improvement in acentric order and thus, poling efficiency ($<\cos^3\theta>/E_{pol}$, where E_{pol} is the poling field strength). Such improvement in acentric order is one of the most straightforward and effective means of improving electro-optic activity because it is not accompanied by an increase in optical loss due to higher absorption as is often encountered with increasing N or β_{zzz}. The focus of this communication is the

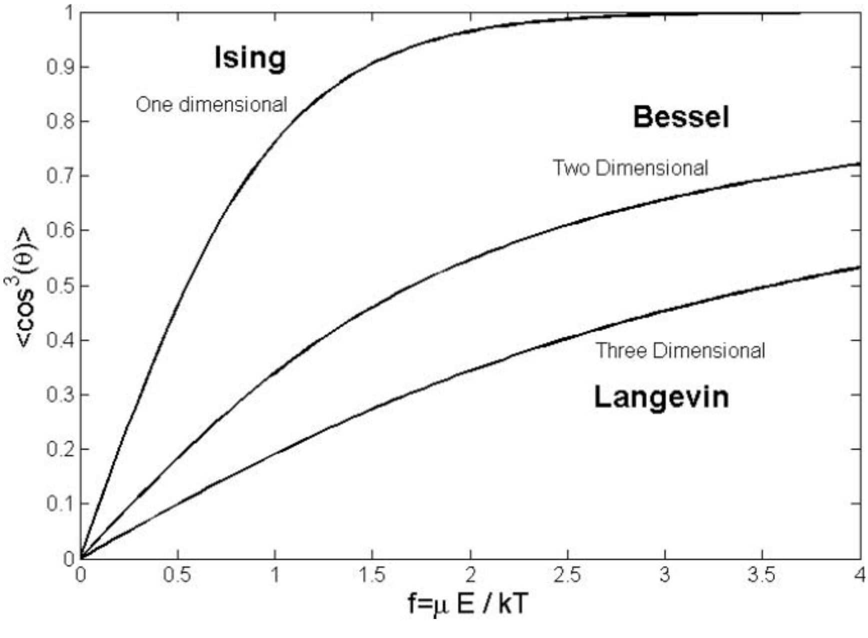

Figure 1. The theoretically-predicted relationship between acentric order and (normalized) electric field poling energy (the product of chromophore dipole moment and the poling field strength divided by thermal energy kT) is shown for different lattice dimensionalities.

increase in acentric order parameter through attachment of pendants (or dendrons) that promote nanoscopic intermolecular cooperativity among the pendant-containing electro-optic chromophores. To the present, such modifications have involved addition of coumarin or arene/perfluoroarene moieties [1]. The former promotes intermolecular cooperativity through dipolar interactions while the latter promotes cooperativity through quadrupolar interactions. The effect of such interactions can be studied through their effect on centric ($<\cos^2\theta>$ or $<P_2>$) and acentric ($<\cos^3\theta>$) order parameters and lattice dimensionality and through their effect on viscoelastic properties. Lattice dimensionality, M, can be approximately related to order parameters through the relationship $<\cos^3\theta>^2 = \{(9 - 2M)/(2 + M)\}<P_2> - \{(3 - M)/2M\}$ where $2<P_2> = 3<\cos^2\theta> - 1$ [14]. More exact calculation of M can be accomplished numerically. The centric order parameter $<\cos^2\theta>$ or $<P_2>$ can be defined by variable angle polarization reference absorption spectroscopy, VAPRAS [15] or by variable angle spectroscopic ellipsometry, VASE [16]. The latter frequently permits determination of the $<P_2>$ order parameter for both EO chromophore and pendant (e.g., the coumarin moiety). Further insight into the effect of molecular cooperativity can be achieved through viscoelastic measurements including shear modulation force microscopy (SM-FM) [17–20], intrinsic friction analysis (IFA) [21, 22], and dielectric relaxation spectroscopy (DRS) [23]. These measurements permit identification of phase transitions associated with molecular cooperativity, entropy changes (ΔS^*) associated with such cooperativity or lattice dimensionality, and the cooperativity length scale (ξ).

Experimental

The molecules and materials studied to the present are shown in Figs. 2–4 and a representative generalized synthetic scheme is shown in Fig. 5. The centric order parameter ($<\cos^2\theta>$ or $2<P_2> = 3<\cos^2\theta> - 1$) is determined by variable angle polarization referenced absorption spectroscopy (VAPRAS) [15] and variable angle spectroscopic ellipsometry (VASE) [16]. VAPRAS is a modification of variable angle polarized absorption spectroscopy (VAPAS) where p-polarized absorption is referenced to s-polarized absorption. This reference method removes many of the experimental artifacts associated with the VAPAS method. Moreover, we employ full Jones matrix analysis [24] to extract the order parameter from raw VAPRAS data. The acentric order parameter ($<\cos^3\theta>$) is determined from electro-optic coefficients measured by attenuated total reflection (ATR) [7,25]. There are two ways that acentric order parameters can be extracted from ATR data. Acentric order parameters are related to the ratio of the two non-zero elements of the electro-optic tensors of OEO materials; namely, $(r_{13}/r_{33}) = (1/2)\{(<\cos\theta>/<\cos^3\theta>) - 1\}$. ATR permits measurement of both elements and the ratio provide a relatively direct route to the determination of the acentric order parameter although theory is required to estimate the ratio of major to minor elements of the molecular first hyperpolarizability tensor. Theory shows that for a 3-D lattice, r_{13}/r_{33} will approximately be equal to 1/3; for a 2-D lattice it will be approximately equal to 1/6; and for a 1-D lattice, the ratio will be approximately equal to 0. Secondly, if β_{zzz} is determined from Hyper Rayleigh Scattering (HRS) [26,27] measurements or can be reliably estimated from theory, then the acentric order parameter can also be determined directly from the measurement of r_{33}. Femtosecond, wavelength-agile HRS measurements were carried out for the chromophores employed in this work [26,27].

Viscoelastic properties are determined by shear modulation force microscopy (SM-FM) [17–20], intrinsic friction analysis (IFA) [21,22], dielectric relaxation spectroscopy (DRS) [23], and differential scanning calorimetry (DSC). SM-FM permits measurement of critical

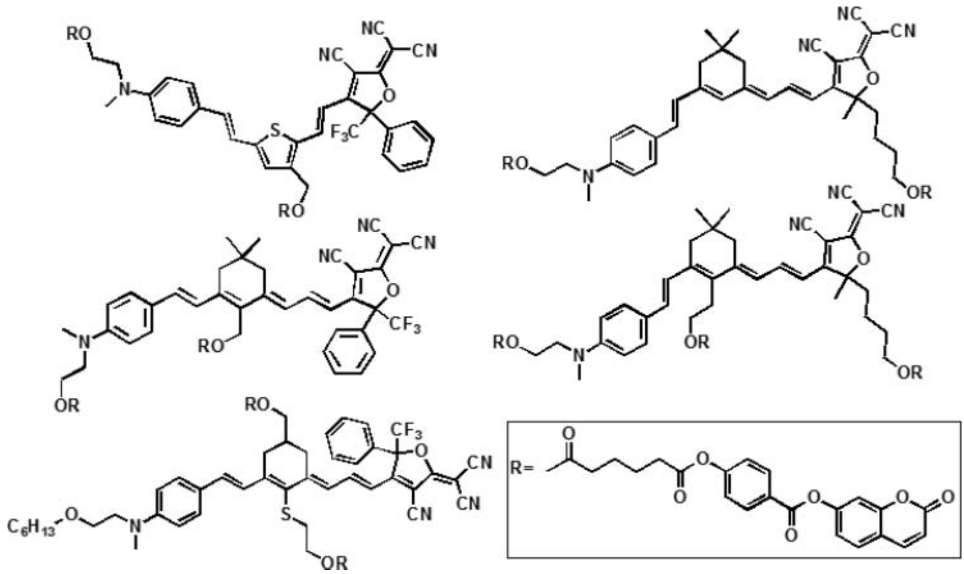

Figure 2. Different chromophore architectures functionalized with coumarin pendant groups. The specific pendant group structure utilized (R) is shown in the box (lower right). The C1 material is shown (upper left). The remaining chromophores depicted represent a comprehensive study of pendant group placement on different positions of the chromophore core as well as exploitation of a chromophore core that has demonstrated a large hyperpolarizability.

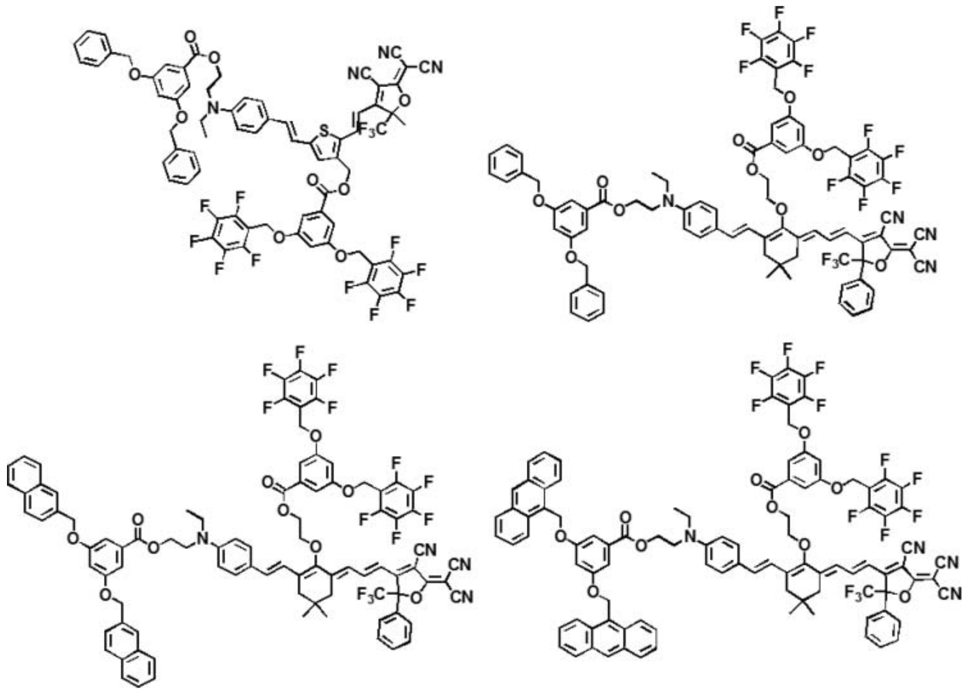

Figure 3. Chromophores with arene-perfluoroarene pendant groups are shown.

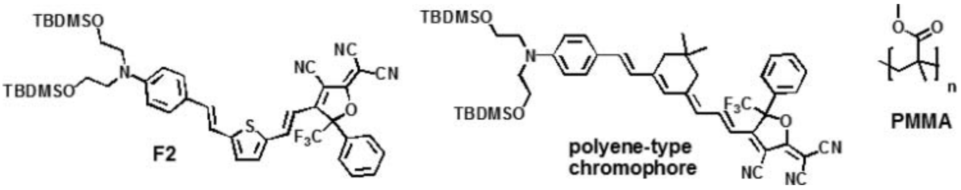

Figure 4. Reference chromophore materials are shown.

temperature values that are indicative of subtle mobility changes. SM-FM data correlates well with macroscopic DSC data but SM-FM reflects a more nanoscopic measurement of viscoelasticity/molecular cooperativity. IFA permits determination of activation entropies (ΔS^*) associated with phase transitions. IFA data can be combined with DRS data to define the length scale of molecular cooperativity, $\xi = \nu_p/f_p$ where ν_p is the velocity peak from IFA and f_p is the frequency peak from DRS for temperature regions where ν_p and f_p data overlap.

Results and Discussion

The ratio of order parameters, $<P_2>/<\cos^3\theta>$, determines lattice dimensionality. For coumarin-containing materials, the lattice dimensionality approaches 2-D [14]. For example, for the C1 material, $<\cos^3\theta> = 0.15 \pm 0.02$, $<P_2> = 0.19 \pm 0.02$, and $M = 2.2$. For the C1 material, the poling efficiency, r_{33}/E_{pol}, is $1.92 \pm 0.04\ (\mathrm{nm/V})^2$. The number density for the C1 material is 4.4×10^{20} molecules/cc. It is useful to compare this material with the core chromophore (F2 of Fig. 4) of the C1 material incorporated into polymethylmethacrylate (PMMA) for a number density of 3.6×10^{20} molecules/cc. For this reference material (F2 in PMMA), $<\cos^3\theta> = 0.015 \pm 0.003$, $<P_2> = 0.04 \pm 0.02$, and $M = 2.8$. Similar lattice dimensionality, M, is observed for lower concentrations of the chromophore/PMMA

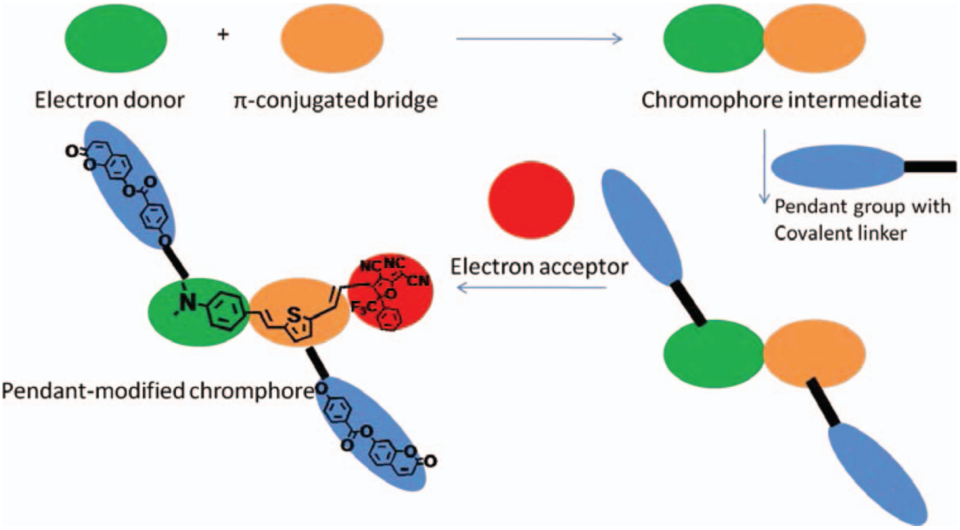

Figure 5. A generic scheme for pendant group-modified chromophore synthesis is illustrated.

composite. For a number density of 3.6×10^{20} molecules/cc, the composite material exhibited a poling efficiency of 0.15 ± 0.02, which is substantially less than that observed for the chromophore modified with coumarin moieties. At lower chromophore concentrations, the poling efficiency of the composite material approaches that of the independent particle limit, namely, $r_{33}/E_{pol} = 0.45 \pm 0.02$ $(nm/V)^2$. Clearly, incorporation of coumarin moieties leads to both reduction in lattice dimensionality and an increase in acentric order (e.g., from 0.07 to 0.15 or approximately a factor of 2). Because of the higher number density that can be achieved for the C1 material (without reduction in poling efficiency) relative to the F2/PMMA reference material, the improvement in poling efficiency is significantly greater than a factor of two.

The SM-FM of the C1 material reveals two temperature transitions (changes in slope of contact stiffness versus temperature). The higher temperature transition corresponds to the material glass transition temperature (T_g). The lower temperature is denoted T_l and the region between T_g and T_l corresponds to a phase of nanoscopic molecular cooperativity or reduced lattice dimensionality. For the C1 material, $T_g = 76 \pm 2°C$ and correlates well with the T_g measured by DSC. For C1, $T_l = 61 \pm 2°C$. IFA indicates that entropy goes through a minimum (order goes through a maximum) in the region between T_l and T_g. The minimum in ΔS^* corresponds to the temperature of optimum poling efficiency. For C1, $|T\Delta S^*|_{max} \sim 56$ kcal. From the correlation of IFA and DRS data, the cooperativity length, $\xi = 55$ nm at 106°C. Unfortunately, 106°C is the lowest temperature at which data is available from both IFA and DRS. This temperature is above the material glass transition so the measured molecular cooperativity length is shorter than that at the temperature for maximum cooperativity. Thus, at the temperature of optimum poling efficiency, the cooperativity length will be considerably greater than 55 nm. The addition of coumarin pendants also improves material photostability as well as influencing thermal transitions [28]. Coumarin moieties can also be photocrosslinked subsequent to electric field poling, thus, increasing the material glass transition temperature [29].

Similar viscoelastic data is observed for analogous arene/perfluoroarene materials suggesting that the strengths of dipolar and quadrupolar interactions deriving from the pendants are comparable. Structural variation of chromophores shown in Figs. 2–4 permits estimation of the various contributions to molecular cooperativity and reduced lattice dimensionality. The greatest contributions clearly arise from the coumarin or arene/perfluoroarene moieties but EO chromophore dipolar interactions also contribute. The pendant interactions make an approximate factor of two greater contribution relative to chromophore dipolar interactions. Diverse van der Waals interactions make a smaller contribution.

Additional improvements to the pendant-modified chromophore architectures can be made to further reduce the dimensionality, thus, increasing acentric order and electro-optic activity. The final electro-optic activity also depends upon the first molecular hyperpolarizability of the core chromophore. Thus, larger electro-optic activity is observed for materials prepared from chromophores containing polyene bridges rather than heteroaromatic bridges. This difference in structure is illustrated in Fig. 4. In addition to hyperpolarizability, the effect of the relative positioning of pendants (or dendrons) on lattice dimensionality or the dimensional character of molecular cooperativity remains to be defined. The detailed effect of the strength of nano-engineered intermolecular electrostatic interactions also remains to be defined. A requirement for choosing the interaction strength of pendants is that introduced interactions do not elevate material glass transition temperatures above material decomposition temperatures or else material melt processability will be lost. For this reason, exploration of ionic and extended hydrogen bonding interactions has not been attractive. However, selective introduction of hydrogen bonding may be of utility.

Guest chromophores can also be added to pendant modified chromophore hosts to exploit the advantages of binary chromophore materials. Indeed, this has been demonstrated using the C1 material as a host. Currently, this approach leads to the largest observed poling-induced electro-optic activity, i.e., values exceeding 300 pm/V (or an order of magnitude greater than lithium niobate) [30].

Conclusions

The nano-engineering of materials described here provides a systematic approach to controlling chromophore order. High chromophore number densities are possible without the deleterious effects of centrosymmetric order observed for chromophore/polymer composite materials. The combination of high order combined with high number densities does create a problem of increased material conductivity at poling temperatures. Such conductivity can reduce poling-efficiency but the effect can be somewhat ameliorated by the introduction of nanoscopic charge blocking (e.g., metal oxide) layers between OEO materials and electrodes [31,32].

The incorporation of coumarin or arene/perfluoroarene moieties leads to nanoscopic molecular cooperativity that increases molecular order and reduces effective lattice dimensionality. This represents the successful introduction of enhanced self-assembly properties into melt-processable soft matter electroactive materials. The reduced lattice dimensionality (approximately 2-D) leads to a two-fold improvement in acentric order in agreement with theoretical predications. Because higher number densities are also possible for the pendant-modified chromophore materials, an even larger enhancement in electro-optic activity is observed relative to that for the same chromophores in chromophore-polymer composite materials. The introduction of specific spatially-anisotropic intermolecular electrostatic interactions that influence lattice dimensionality and acentric order has provided a route to optimization of organic electro-optic materials leading to optimum electro-optic activity and photochemical stability. An even greater improvement in acentric order could be achieved if lattice dimensionality could be further reduced to values between 2-D and 1-D.

Acknowledgments

The authors acknowledge financial support for this research from the National Science Foundation (DMR00905686) and the Air Force Office of Scientific Research (FA9550-09-1-0589). The authors also wish to thank members of Robinson, Overney, Jen, Reid, and Dalton research groups at the University of Washington for many helpful discussions and with assistance with calculations and measurements.

References

[1] Dalton, L. R. et al. (2011). *Chem. Mater.*, *23*, 430.
[2] Dalton, L. R. et al. (1997). *Proc. Natl. Acad. Sci. USA*, *94*, 4842.
[3] Benight, S. J. et. al. (2009). *J. Mater. Chem.*, *19*, 7466.
[4] Robinson, B. H., & Dalton, L. R. (2000). *J. Phys. Chem. A*, *104*, 4785.
[5] Leahy-Hoppa, M. R. et al. (2006). *J. Phys. Chem. A*, *110*, 5792.
[6] Dalton, L. R. et al. (2003). *Opt. Mater.*, *21*, 19.
[7] Dalton, L. R. et al. (2010). *Chem. Rev.*, *110*, 25.
[8] Sullivan, P. A. et al. (2007). *J. Amer. Chem. Soc.*, *129*, 7523.
[9] Sullivan, P. A. et al. (2009). *J. Phys. Chem. B*, *113*, 15581.

[10] Pereverzev, Y. Y. et al. (2008). *J. Phys. Chem. C*, *112*, 4355.
[11] Olbricht, B. C. et al. (2008). *J. Phys. Chem. C*, *112*, 7983.
[12] Shi, Y. et al. (2000). *Science*, *288*, 119.
[13] Kim, T.-D. et al. (2008). *J. Phys. Chem. C*, *112*, 8091.
[14] Benight, S. J. et. al. (2010). *J. Phys. Chem. B*, *114*, 11949.
[15] Olbricht, B. C. et al. (2011). *J. Phys. Chem. B*, *115*, 231.
[16] Woollam, J. A. (1999). In: *Optical Metrology*, Vol. CR72, SPIE: Bellingham, WA, 3.
[17] Gray, T. et al. (2008). *Nano Lett.*, *8*, 754.
[18] Ge, S. et al. (2000). *Phys. Rev. Lett.*, *85*, 2340.
[19] Dinelli, F. et al. (2000). *J. Chem. Phys.*, *113*, 2043.
[20] Wei, J. H. (2006). *J. Membrane Sci.*, *279*, 608.
[21] Overney, R. M. (1994). *Phys. Rev. Lett.*, *72*, 3546.
[22] Knorr, D. B. J. et al. (2009). *Ultramicroscopy*, *109*, 991.
[23] Hedvig, P. (1977). *Dielectric Spectroscopy of Polymers*, John Wiley & Sons: New York, NY.
[24] Mansuripur, M. (1990). *J. Appl. Phys.*, *67*, 6466.
[25] Davies, J. A. et al. (2008). *J. Am. Chem. Soc.*, *130*, 10565.
[26] Firestone, K. A. et al. (2005). *Proc. SPIE*, *5935*, 59350P1.
[27] Bale, D. et al. (2011). *J. Phys. Chem. B*, *115*, 3505.
[28] Benight, S. J. et al. (2010). Proc. SPIE, 7774, DOI: 10.1117/12.862059.
[29] Tian, Y. et al. (2003). *J. Polym. Sci., Part A: Polym. Chem.*, *41*, 2197.
[30] Zhou, X.-H. et. al. (2009). *Adv. Mater.*, *21*, 1976.
[31] Sprave, M. et. al. (1996). *Appl. Phys. Lett.*, *69*, 2962.
[32] Huang, S. et. al. (2010). *Appl. Phys. Lett.*, *96*, 243311.